# The two sides of the coin of psychosocial stress: evaluation by positron emission tomography

Kopschina Feltes, Paula

# Glial, metabolic and behavioral response to recurrent psychosocial stress: PET imaging in stress-sensitized and stress-naïve aged rats

Author(s): Paula Kopschina Feltes, Janine Doorduin, Luis Eduardo Juárez-Orozco LE, David Vállez García, Rudi AJO Dierckx, Cristina M. Moriguchi-Jeckel, Erik FJ de Vries.

CHAPTER 5

In preparation for submission.

**Abstract**

***Background:*** Early life adversities increases the vulnerability to psychiatric conditions later in life. However, it is still unknown how stress exposure influences the neurobiological response to a secondary stressful event at an older age. The present study aimed to evaluate glial, brain-metabolic and behavioral response to repeated social defeat (RSD) in stress-sensitized (SS, previously exposed to 5-day RSD protocol during adolescence) and stress-naïve (SN) aged rats through positron emission tomography (PET).

***Methods:*** Fourteen-month old SN (n=8) and SS (n=10) Wistar rats underwent a 5-day RSD protocol, repeated PET imaging with $^{11}$C-PBR28 (glial activation) and $^{18}$F-FDG (brain metabolism), and behavioral and biochemical assessments.

***Results:*** RSD at old age induced anhedonic-like behavior in SS rats only, while anxiety was present in both groups. RSD in aged SN rats increased corticosterone levels, whereas recurrence of RSD blunted the corticosterone response in SS rats. RSD increased $^{11}$C-PBR28 uptake levels in SN rats, whereas re-exposure to RSD diminished tracer uptake in the brain of SS rats. Higher brain levels of the cytokines IL-1β and IL-10 were found in SN rats after RSD, as compared to SS rats. RSD caused hypometabolism in the brains of both groups.

***Conclusion:*** Recurrence of RSD in aged SS rats induced depressive- and anxiety-like behavior, despite diminished corticosterone and brain inflammatory responses, as compared to SN rats. In contrast to SN rats, the immune response in SS rats was not correlated with corticosterone levels, pointing towards an alternative pathway for coping with detrimental stressful stimuli or exhaustion of the brain immune cells in sensitized animals.

**Keywords:** chronic stress, neuroinflammation, brain metabolism, PET imaging, repeated social defeat.

**Introduction**

Psychosocial stress is a predominant environmental risk factor for several psychiatric disorders, including major depressive disorder (MDD) (1). It is estimated that 20-25% of individuals exposed to highly stressful events develop MDD (2). Interestingly, trauma exposure at a young age increases the likelihood of fulfilling the criteria for MDD at any point in life (3). It has been hypothesized that such exposures may modify the individual's immune, endocrine, neural and behavioral responsiveness to recurrent stressful conditions at later ages (4).

Stimuli such as chronic stress can activate microglia and astrocytes, the brain's immune cells, which can subsequently release pro-inflammatory cytokines, such as interleukin-1β (IL-1β), interleukin-6 (IL-6) and tumor necrosis factor-α (TNF-α) (5). Pro-inflammatory cytokines produced during glial activation might influence central levels of neurotransmitters (6). In addition, stress-induced activation of the hypothalamic-pituitary-adrenal (HPA) axis can cause an increase in glucocorticoid levels. These glucocorticoids can cross the blood-brain barrier (6) and act on receptors located in vulnerable brain regions. The brain is highly sensitive to stress and altered glucocorticoid levels during crucial periods of development (such as adolescence), mainly in brain areas as the medial prefrontal cortex (MPFC), cingulate cortex and orbitofrontal cortex (OBFC) (7). Interestingly, the prefrontal cortex (PFC) shows higher levels of glucocorticoid receptor mRNA in adolescence than during any other period of development (8), suggesting that the PFC may be especially sensitive to glucocorticoid regulation during this period. The aforementioned stress-sensitive brain regions are amply associated with reward, emotional regulation, and fear extinction and therefore appear to be of relevance for stress recovery (7). Negative neurobiological changes during developmental periods might have long-lasting detrimental effects and increase vulnerability to depression (9). As a potential reflection of these detrimental effects, stress has been found to decrease brain metabolism in several brain regions in animal models of stress (10). Notably, a similar decrease in brain metabolism is also found in patients with unipolar depressive disorder (11–14). Hence, immune activation and cytokine release in the central nervous system and abnormalities in the HPA axis have been suggested as key factors in the development and recurrence of depression (15). Although these mechanisms may not apply to all patients, they may be of particular interest for the subgroup of treatment-resistant MDD patients (6).

The repeated social defeat (RSD) rat model has been widely used to mimic psychosocial stress in rodents, due to its high ethological validity (16; 17). RSD is able to provoke immune dysregulation, coupled with depressive- and anxiety-like behavior that resembles the MDD phenotype. Previous studies in adolescent rats demonstrated glial (mainly microglia) activation in response to RSD, in conjunction with an elevation of pro-inflammatory cytokine levels (18–20). These alterations were transient and resolved within a month (21; 22). However, such a stressful event may have primed pro-inflammatory microglial responses to a subsequent stress exposure (23). Consequently, transient effects of psychosocial stress early in life may translate into long-term (persistent) immunological, behavioral and brain metabolic disturbances, as the ones observed in (treatment-resistant) MDD patients. However, there is still no evidence available that supports such conjecture. Furthermore, it is also unknown whether an early exposure to psychosocial stress would influence the response to a secondary stressful event later in life.

Therefore, the aim of the present study was to evaluate the glial, brain-metabolic and behavioral response to repeated social defeat (RSD) in 1) stress-sensitized (SS) (i.e. with a history of previous exposure to psychosocial stress during adolescence) and 2) stress-naive (SN) aged rats through repeated neuroimaging. Positron emission tomography (PET) offers the opportunity to longitudinally image the (patho)physiological processes that are seemingly altered in MDD patients and animal models. PET has been successfully used to evaluate glial activation (24) with the translocator protein receptor (TSPO) tracer $^{11}$C-PBR28 (25), and to assess brain glucose metabolism (11) with the glucose analogue 2'-[$^{18}$F]fluoro-2'-deoxyglucose ($^{18}$F-FDG).

## Materials and Methods

### *Experimental Animals*

Male outbred Wistar Unilever rats of fourteen months were used for the present study (n=18, 577±11g). They were purchased at the age of seven weeks from Harlan Laboratories (Horst, The Netherlands) and were allowed to age under monitored conditions during twelve months. Rats were kept in humidity-controlled, thermo-regulated (21±2°C) rooms under a 12:12 hour light:dark cycle with lights on at 7 a.m. Rats had *ad libitum* access to food and water. During the RDS protocol, rats were housed individually and divided into two groups: stress-naïve (SN, n=8) and stress-sensitized (SS, n=10) rats.

Animal experiments were performed in accordance with Dutch Regulations for Animal Welfare. All procedures were approved by the Institutional Animal Care and Use Committee of the University of Groningen (protocol DEC 6828A and 6828B).

***Study design***

The overall design of the study is depicted in Fig. 1. SS rats were subjected to five consecutive days of RSD when they were eight weeks old (22). During the RSD protocol, both groups were handled similarly. However, SN rats were only placed in another cage, but not exposed to an aggressive resident rat. After the RSD protocol at adolescence, rats were allowed to age for 12 months and housed in pairs to prevent isolation stress (26; 27). At the age of 14 months, rats from both groups (SN and SS) underwent a 5-day RSD protocol (day 0–4), PET scans with $^{11}$C-PBR28 and $^{18}$F-FDG (days -1, 6, 11 and 25), behavioral tests and biochemical assessments. Body weight was measured daily between day 0 and 25. On day 25, the rats were terminated and the brains were collected for the quantification of pro- and anti-inflammatory cytokines.



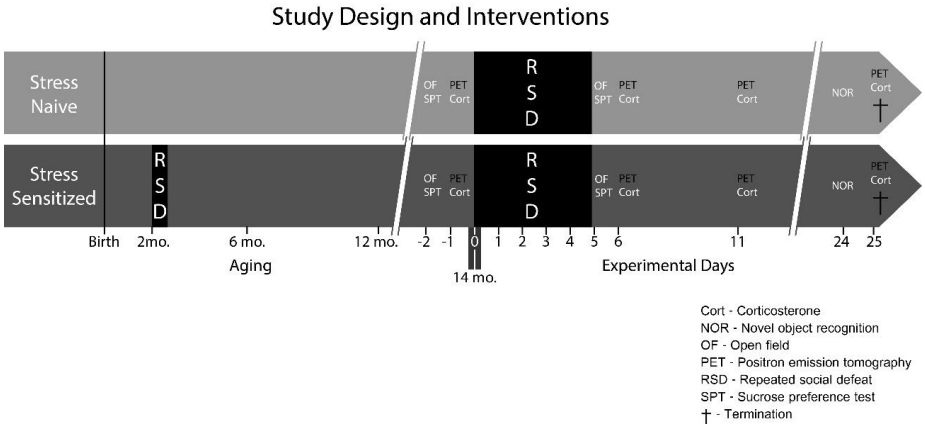


**Figure 1:** Stress-naïve (SN) and stress-sensitized (SS) rats were subjected to a 5-day RSD protocol (day 0–4) at the age of 14 months. PET scans with $^{11}$C-PBR28 and $^{18}$F-FDG were conducted on experimental days -1, 6, 11 and 25. In order to evaluate post-RSD behavioral alterations, the sucrose preference test (SPT) and open field (OF) were conducted on days -2 and 5. Corticosterone levels were assessed on days -1, 6, 11 and 25. On day 25, after the PET scans, rats were terminated and the brains were collected for the quantification of pro- and anti-inflammatory cytokines.

***Repeated Social Defeat***

RSD was carried out through the introduction of SN and SS rats (intruder) into the cage of a dominant (resident) male outbred Long Evans rat (537±28g; Harlan, Indianopolis,

USA). All the intruders were exposed to the same residents (using a different resident for each social defeat conflict to avoid habituation). The male Long Evans rats were housed in a separate experimental room in large cages (80x50x40 cm) with a tubal ligated Long Evans female rat to stimulate territorial aggression (16). The Long Evans residents were screened for aggressive behavior at least three times prior to the experiment (28; 29). Only residents with an attack latency shorter than 30 s were used for the actual social defeat experiment (30).

The social defeat experiment was conducted as previously described (16), and it always took place between 16:00–18:00 p.m. Briefly, the females were removed from the cage of the resident before the introduction of the experimental rat (intruder). The total duration of the interaction between the resident and the intruder was of 60 min, but the physical interaction was limited to a maximum period of 10 min, or shorter, if the intruder assumed a supine (submissive) position for at least 3 seconds. Hereafter, the intruder was placed in a wire mesh cage inside the cage of the resident to avoid further physical contact, but still allowing intense visual, auditory and olfactory interactions for the remainder of the 60-min stress period. The social defeat protocol was repeated on 5 consecutive days using different residents.

***Body weight gain***

Body weight gain was calculated individually for each rat as the difference between the body weight at a certain time point minus the body weight on experimental day 0 (first day of RSD).

***Behavioral Tests***

To assess RDS-induced behavioral changes, the open field (anxiety, locomotion) (31), novel object recognition (visual memory) (32) and sucrose preference test (anhedonia) (29) were performed. The open field and novel object recognition tests were recorded on video for further analysis using Ethovision XT8.5 software (Noldus Information Technology, Wageningen, The Netherlands).

*Open field (OF)*

Rats were placed inside a square box (100x100x40 cm) for 10 min. The time spent in the center of the arena relative to the time spent at the borders (anxiety), and the total distance moved (locomotion) were documented.

*Novel object recognition (NOR)*

On day 24, rats were placed in a square box (50x50x40 cm) with two identical objects (plastic bottles or Lego cubes) (33; 34). They were allowed to explore the objects for 3 min. The objects were removed and after 2 h one familiar and one new object were presented to the rat for 3 min. The preference index (PI) was calculated as the ratio between time spent on exploring the new object and the total time spent on object exploration.

*Sucrose Preference (SPT)*

Rats were habituated to a 1% sucrose solution for 1h during 4 days prior to the experiment. At baseline and after 5 days of RSD, rats were exposed to two bottles placed randomly in the cage, one containing water and one with 1% sucrose. Preference for sucrose was calculated as the total intake of sucrose solution divided by the total liquid intake and multiplied by 100% (29; 35).



***Corticosterone Levels***

For determination of corticosterone levels, rats were anesthetized with isoflurane mixed with oxygen and 0.5 mL of whole blood was quickly collected from the tail vein on day -1, 6, 11 and 25. Samples were always collected at 10 a.m. to avoid circadian fluctuations. The blood was allowed to clot for 15 min and centrifuged at 6.000 rpm (3.5g) for 8 min at room temperature to obtain serum samples. Samples were stored at -20°C until further analysis by radioimmunoassay. Corticosterone (Sigma Chemical Co., Missouri, USA.) was used as standard and $^{3}$H-corticosterone as tracer (Perkin & Elmer, Massachusetts, USA).

***PET***

PET scans were performed using a small animal PET scanner (Focus 220, Siemens Medical Solutions, USA). $^{11}$C-PBR28 PET scans were always carried out in the morning. The rats were anesthetized with isoflurane mixed with oxygen (5% for induction, 2% for maintenance) and $^{11}$C-PBR28 was injected via the penile vein (73±34 MBq, 1.25±1.91 nmol). Immediately after injection, rats were allowed to wake up and recover in their home cage. Rats were anesthetized 45 min after tracer injection and placed in prone position into the camera with the head in the field of view. A 30-min static scan was

acquired. The body temperature was maintained at 37°C with heating pads, heart rate and blood oxygen saturation were monitored, and eye salve was applied to prevent conjunctival dehydration. After completion of the emission scan, a transmission scan was obtained using a $^{57}$Co point source enabling attenuation and scatter correction of PET images.

After at least 10 half-lives of the radioisotope $^{11}$C, a $^{18}$F-FDG PET scan was acquired. Between scans, rats were deprived of food for 4-6 h. Rats were injected intraperitoneally (36; 37) with $^{18}$F-FDG (27±5 MBq) and returned to their home cage. After 45 min, $^{18}$F-FDG PET acquisition was performed as described above for $^{11}$C-PBR28 PET.

The reconstruction of the scans was performed iteratively (OSEM2D, 4 iterations and 16 subsets) into a single frame after being normalized and corrected for attenuation and decay of radioactivity. Images with a 128x128x95 matrix, a pixel width of 0.632 mm, and a slice thickness of 0.762 mm were obtained. PET images were automatically co-registered to a functional $^{11}$C-PBR28 or $^{18}$F-FDG rat brain template (25; 38), using PMOD 3.6 software (PMOD technologies Ltd., Switzerland). Aligned images were resliced into cubic voxels (0.2 mm) and converted into standardized uptake value (SUV) images: SUV = [tissue activity concentration (MBq/g) x body weight (g)] / [injected dose (MBq)], assuming a tissue density of 1g/mL. $^{18}$F-FDG uptake was not corrected for blood glucose levels (39).

Tracer uptake was calculated in several predefined volumes-of-interest (VOI). VOIs were selected based on previous findings (11; 18; 24; 40–45), taking the size of the brain regions into consideration. Small brain regions were excluded to minimize partial volume effects (47). The investigated regions were the amygdala/piriform complex, brainstem, cerebellum, cingulate cortex, entorhinal cortex, frontal association cortex (FCA), hippocampus, hypothalamus, insular cortex, MPFC, motor/somatosensory cortex, OBFC, and striatum.

***Enzyme linked immunoassay (ELISA) for pro-inflammatory cytokines in the brain***

On day 25, rats were terminated under deep anesthesia by transcardial perfusion with phosphate-buffered saline pH 7.4. Brains were collected and rapidly frozen and stored at -80°C. Frontal cortex, hippocampus, cerebellum and parietal/temporal/occipital cortex were dissected and prepared as published (34). IL-6, IL-1β, and IL-10 (Thermo Scientific, Rockford, USA) concentrations were determined in these brain regions by ELISA

according to the manufacturer's instructions and the cytokine levels were corrected for the amount of proteins, as determined through a Bradford Assay.

***Statistical Analysis***

Statistical analyses were performed with IBM SPSS 23 software (IBM Corp, New York, USA). Continuous data are expressed as mean ± standard error of the mean (SEM). The Generalized Estimating Equations (GEE) model (48) was used for statistical analysis of body weight measurements, behavioral tests (OF and SPT), corticosterone levels, and PET data, in order to account for repeated measurements in the longitudinal design and missing data. The parameters "group", "day of measurement" and the interaction "group × day of measurement" were included as independent variables for the statistical analysis of body weight gain, corticosterone levels, and the behavioral tests. For the statistical analysis of $^{11}$C-PBR28 and $^{18}$F-FDG uptake (SUV), the GEE model was applied independently for each brain region, using the variables "group", "day of scan" and the interaction "group × day of scan" in the model. The data was further explored through pairwise comparison of "group × day of scan" in each brain region for all scan time points combined. The AR(1) working correlation matrix was selected according to the quasi-likelihood under the independence model information criterion value. Wald's statistics and associated *p*-values were considered statistically significant if $p<0.05$, after the sequentially rejective Bonferroni-Holm correction for multiple comparisons was applied to ensure that the Type I error resulting from multiple tests never exceeded the *p* set level of statistical significance at $\alpha= 0.05$ (49; 50). Spearman correlations were performed to investigate the relationship between corticosterone levels, cytokines, behavior and tracer uptake levels between groups at different timepoints. Between-group differences in the PI (NOR) and brain cytokines levels were assessed through the Mann-Whitney U test and the results were reported as the median and the 0.25-0.75 interquartile range (IQR).

**Results**

*RSD significantly decreases body weight gain*

No statistically significant difference in body weight between groups was found before the start of RSD (SN: 571±19 vs. SS: 581±12, $p=0.66$). The GEE analysis revealed a significant main effect for the factor "day of measurement" ($p<0.001$) and the interaction "day of measurement x group" ($p<0.001$), but not for "group". Pairwise analysis of the

data revealed between-group differences on experimental days 1 to 3 only, indicating that RSD affected body weight significantly more in SS rats than in SN rats (day 3, SN: -3.6±1.4g, vs. SS: -8.1±0.8g, $p$=0.007). From experimental day 4 onwards, no significant difference in body weight gain between groups was observed anymore (Fig. 2).

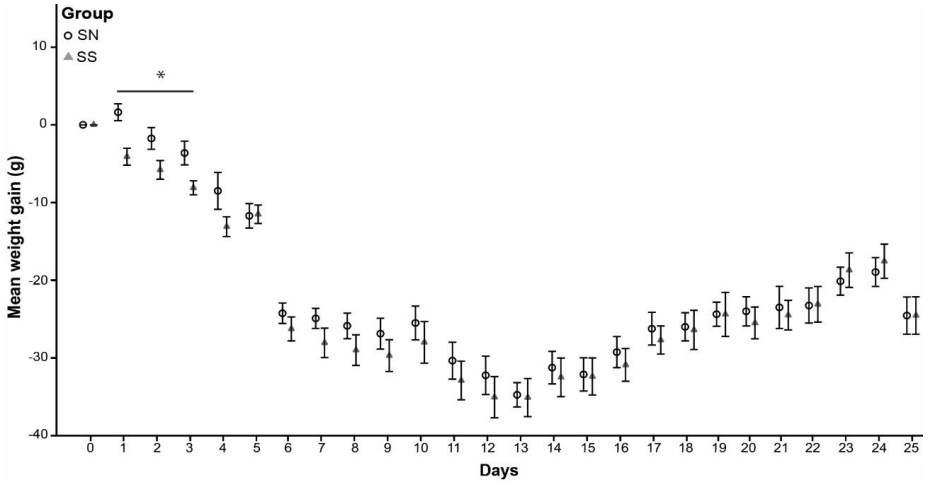


**Figure 2:** Body weight gain (g) of stress-naïve (SN) and stress-sensitized (SS) rats during the 25 days of the study protocol. Significant differences between the groups were apparent from day 1 to 3, with SS rats gaining less weight than SN rats ($p$<0.05). From day 4 onwards, both groups gained weight at the same rate, without returning to baseline levels until the end of the study. The dips in body weight gain on day 6, 11 and 25 are due to the PET procedures on these days. *$p$<0.05.

*RSD induces anxiety-like behavior and decreases locomotor activity both in SN and SS rats, whereas RSD-induced anhedonia is only observed in SS rats*

No significant differences in sucrose preference between groups were found at baseline. RSD provoked anhedonia in SS rats, as it reduced the sucrose preference from 93±2% on day -2 to 69±7% on day 5 ($p$=0.003). In contrast, no significant change in sucrose preference was observed after RSD in SN rats (90±4% to 84±5%, $p$=0.25). A trend towards significance was observed in the between-groups comparison on day 5 ($p$=0.060) (Fig. 3-A).

The anxiety-like behavior and locomotor activity were assessed with the OF test at baseline and after the RSD protocol (day 5). At baseline, SN rats moved a total distance of 2.2±0.5 m and spent 64±20 s in the center of the arena, whereas after RSD the total distance moved was reduced to 1.3±0.3 m ($p$<0.001) and the time spent in the center to 19±11s ($p$=0.016). A similar pattern was observed in SS rats, with a distance moved of

2.4±0.2 m and a time spent in the center of 43±9 s at baseline. On day 5, these measures were significantly reduced to 1.4±0.1 m and 9±2 s ($p$<0.001), respectively. No significant differences in locomotion or the time spent in the center were observed between both groups, neither at baseline, nor on day 5 (Fig. 3-B, C).

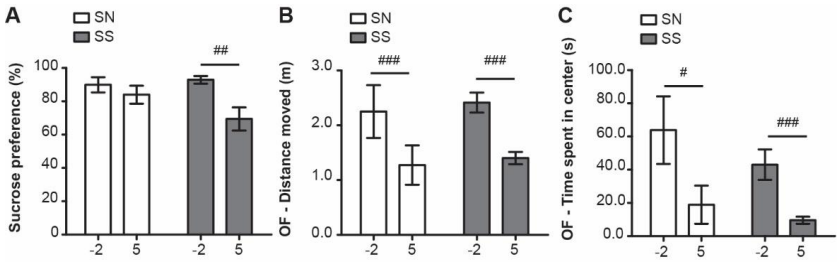


**Figure 3:** RSD-induced behavioral alterations in both SN and SS rats. **A:** Within-group comparison between baseline and day 5 showed anhedonic-like behavior through the sucrose preference test (SPT) in SS rats ($p$<0.01), but not in SN rats. $^{\#\#}p$<0.01. **B:** Anxiety-like behavior was demonstrated in both SN and SS rats in the open field test (OF), with a decreased distance moved on day 5 as compared to baseline ($p$<0.001) and **C:** decreased total time spent in the center of the arena. SS rats had a more pronounced decrease in total time spent in the center $p$<0.001 on day 5 when compared to baseline, than SN rats ($p$<0.05). $^{\#}p$<0.05 and $^{\#\#\#}p$<0.001.



To evaluate effects on long-lasting memory impairment, the NOR test was performed on day 24. No significant differences in the PI were found between groups (SN: 48%, IQR 43-61 *vs.* SS: 56%, IQR 46-70, $p$=0.33).

*RSD provokes a generalized decrease in glucose metabolism*

No significant differences in brain glucose metabolism between SN and SS rats were found at baseline. On day 11, however, $^{18}$F-FDG PET revealed several brain regions with lower glucose metabolism in SS rats than in SN rats. The affected brain regions were the amygdala (-58%, $p$<0.001), brainstem (-62%, $p$<0.001), cerebellum (-39%, $p$=0.002), entorhinal cortex (-69%, $p$<0.001), hippocampus (-35%, $p$=0.012), hypothalamus (-44%, $p$=0.001), insular cortex (-51%, $p$<0.001), OBFC (-36%, $p$=0.008) and striatum (-48%, $p$<0.001). On day 6 and 25, no significant differences in $^{18}$F-FDG uptake between SS and SN rats were observed in any brain region anymore.

A within-group analysis was conducted to explore the effect of RSD on glucose metabolism over time, relative to baseline levels (Fig.4). SN rats did not show any significant effect of RSD on day 6 and 11, but had a general decrease in tracer uptake in the brain on day 25. The affected brain regions in SN rats were the amygdala (-13%, $p$=0.004), brainstem (-11% $p$=0.048), cerebellum (-11%, $p$=0.026), entorhinal cortex (-

16%, $p$=0.001), FCA (-12%, $p$=0.021), hippocampus (-12%, $p$=0.017), hypothalamus (-12%, $p$=0.02), insular cortex (-13%, $p$=0.014), motor / somatosensory cortex (-13%, $p$=0.009), and striatum (-10%, $p$=0.036). On the other hand, SS rats did not show any significant changes in $^{18}$F-FDG uptake on day 6 and 25, but presented a large generalized decrease in glucose metabolism only on day 11. The brain regions of SS rats with decreased uptake on day 11 compared to baseline were the amygdala (-60%, $p$<0.001), brainstem (-64%, $p$<0.001), cerebellum (-38%, $p$<0.001), entorhinal cortex (-70%, $p$<0.001), hippocampus (-37%, $p$<0.001), hypothalamus (-48%, $p$<0.001), insular cortex (-53%, $p$<0.001), MPFC (-22%, $p$<0.001), OBFC (-36%, $p$<0.001) and striatum (-52%, $p$<0.001) (Table 1).

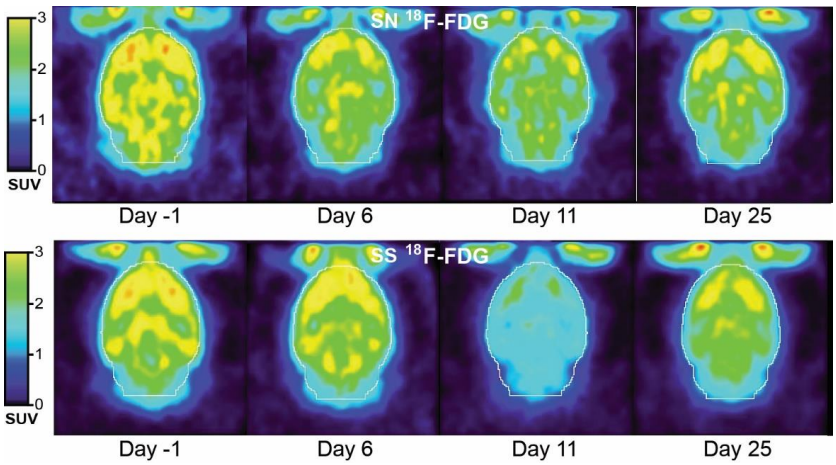


**Figure 4:** Representative $^{18}$F-FDG PET images from SN and SS rats on day -1, 6, 11 and 25.

When investigating the correlation between regional $^{18}$F-FDG uptake and behavioral alterations, no significant correlations were found at all.

**Table 1** – $^{18}$F-FDG SUV between-group comparison for individual brain regions of stress-naïve (SN, n=8) and stress-sensitized (SS, n=10) rats at baseline, day 6, 11 and 25.

| | Baseline | | | Day 6 | | | Day 11 | | | Day 25 | | |
|---|---|---|---|---|---|---|---|---|---|---|---|---|
| | SN | SS | | SN | SS | | SN | SS | | SN | SS | |
| **Brain Regions** | Mean ± SE | Mean ± SE | *p* | Mean ± SE | Mean ± SE | *p* | Mean ± SE | Mean ± SE | *p* | Mean ± SE | Mean ± SE | *P* |
| Amygdala/Piriform complex | 2.35 ± 0.14 | 2.42 ± 0.13 | n.s | 2.08 ± 0.1 | 2.24 ± 0.12 | n.s | 2.28 ± 0.28 | 0.96 ± 0.10 | <0.001 | 2.04 ± 0.08 | 2.29 ± 0.16 | n.s |
| Brainstem | 2.40 ± 0.14 | 2.45 ± 0.14 | n.s | 2.16 ± 0.12 | 2.37 ± 0.12 | n.s | 2.38 ± 0.30 | 0.87 ± 0.07 | <0.001 | 2.13 ± 0.06 | 2.42 ± 0.17 | n.s |
| Cerebellum | 2.40 ± 0.15 | 2.37 ± 0.12 | n.s | 2.10 ± 0.09 | 2.25 ± 0.10 | n.s | 2.40 ± 0.27 | 1.47 ± 0.15 | 0.002 | 2.11 ± 0.07 | 2.28 ± 0.14 | n.s |
| Cingulate cortex | 3.09 ± 0.22 | 3.05 ± 0.22 | n.s | 2.68 ± 0.12 | 2.80 ± 0.18 | n.s | 3.07 ± 0.40 | 2.97 ± 0.34 | n.s | 2.77 ± 0.11 | 2.93 ± 0.23 | n.s |
| Entorhinal cortex | 2.41 ± 0.14 | 2.44 ± 0.14 | n.s | 2.08 ± 0.11 | 2.23 ± 0.14 | n.s | 2.33 ± 0.32 | 0.73 ± 0.07 | <0.001 | 2.03 ± 0.08 | 2.28 ± 0.16 | n.s |
| Frontal association cortex | 3.27 ± 0.22 | 3.08 ± 0.18 | n.s | 2.88 ± 0.15 | 2.87 ± 0.15 | n.s | 3.20 ± 0.37 | 2.89 ± 0.33 | n.s | 2.87 ± 0.13 | 2.92 ± 0.19 | n.s |
| Hippocampus | 2.68 ± 0.16 | 2.68 ± 0.15 | n.s | 2.37 ± 0.11 | 2.53 ± 0.13 | n.s | 2.61 ± 0.32 | 1.69 ± 0.18 | 0.012 | 2.35 ± 0.09 | 2.62 ± 0.20 | n.s |
| Hypothalamus | 2.32 ± 0.14 | 2.36 ± 2.2 | n.s | 2.07 ± 0.12 | 2.20 ± 0.11 | n.s | 2.20 ± 0.27 | 1.23 ± 0.11 | 0.001 | 2.03 ± 0.07 | 2.25 ± 0.15 | n.s |
| Insular cortex | 3.07 ± 0.19 | 3.08 ± 0.17 | n.s | 2.64 ± 0.11 | 2.84 ± 0.16 | n.s | 2.98 ± 0.34 | 1.45 ± 0.16 | <0.001 | 2.66 ± 0.11 | 2.95 ± 0.21 | n.s |
| Medial Prefrontal cortex | 3.18 ± 0.21 | 3.20 ± 0.21 | n.s | 2.84 ± 0.11 | 2.95 ± 0.17 | n.s | 3.11 ± 0.42 | 2.51 ± 0.29 | n.s | 2.88 ± 0.12 | 3.07 ± 0.25 | n.s |
| Motor/Somatosensory cortex | 2.94 ± 0.19 | 2.74 ± 0.17 | n.s | 2.51 ± 0.11 | 2.51 ± 0.14 | n.s | 2.90 ± 0.34 | 2.53 ± 0.30 | n.s | 2.56 ± 0.10 | 2.61 ± 0.16 | n.s |
| Orbitofrontal cortex | 3.51 ± 0.21 | 3.40 ± 0.21 | n.s | 3.11 ± 0.12 | 3.15 ± 0.17 | n.s | 3.41 ± 0.40 | 2.18 ± 0.25 | 0.008 | 3.19 ± 0.15 | 3.29 ± 0.24 | n.s |
| Striatum | 2.78 ± 0.17 | 2.96 ± 0.17 | n.s | 2.49 ± 0.1 | 2.76 ± 0.14 | n.s | 2.72 ± 0.34 | 1.41 ± 0.15 | <0.001 | 2.49 ± 0.09 | 2.90 ± 0.23 | n.s |

*RSD induces a different glial activation pattern in SS rats than in SN rats*

A between-group comparison of the $^{11}$C-PBR28 PET data revealed significant differences in tracer uptake between groups at baseline (day -1) in several brain regions. Increased $^{11}$C-PBR28 uptake was found in the cerebellum (+30%, $p$<0.001), cingulate cortex (+30%, $p$=0.003), FCA (+30%, $p$=0.003), MPFC (+46%, $p$<0.001) and OBFC (+44%, $p$<0.001) of SS rats, as compared to SN rats. $^{11}$C-PBR28 uptake at baseline was significantly lower in the entorhinal cortex (-14%, $p$=0.001) and hypothalamus (-26%, $p$<0.001) of SS rats than in SN rats. Smaller differences were found on day 6 and 25. On day 6, SS rats had a significantly increased uptake only in the cerebellum (+27%, $p$=0.023), whereas on day 25 SS rats even had significantly lower tracer uptake than SN rats in the cingulate cortex (-23%, $p$=0.024), hypothalamus (-25%, $p$=0.045) and motor / somatosensory cortex (-25%, $p$=0.012).

A within-group comparison (Table 2) demonstrated that SN rats presented an increase in $^{11}$C-PBR28 uptake over time, which became significant 7 days after RSD (day 11) and persistent until the end of the experiment (day 25) in the cingulate cortex (+22%, $p$=0.022; and +45%, $p$<0.001, respectively), MPFC (+26, $p$<0.001; and +44%, $p$<0.001) and OBFC (+18%, $p$<0.001; and 40%, $p$=0.001), when compared to baseline. Three weeks after RSD (day 25), tracer uptake was also significantly increased in the FCA (25%, $p$=0.012). Conversely, a significant decrease in $^{11}$C-PBR28 uptake was observed on day 6 in the brainstem (-25%, $p$=0.006), hippocampus (-29%, $p$<0.001), hypothalamus (-40%, $p$<0.001), insular cortex (-18%, $p$=0.008), motor/somatosensory cortex (-14%, $p$=0.039) and striatum (-27%, $p$<0.001), followed by normalization to baseline levels up to day 25. The entorhinal cortex also presented a decrease in uptake on day 6, but without recovery until the end of the experiment (-33%, $p$<0.001).

Taken together, these results suggest a migration of activated glia to RSD affected regions, followed by recovery in almost all glial depleted regions.

**Table 2 –** $^{11}$C-PBR28 SUV within-group comparison for individual brain regions of stress-naïve (SN, n=8) and stress-sensitized (SS, n=10) rats at baseline, day 6, 11 and 25.

| | SN | | | | | | | | SS | | | | | | | |
|---|---|---|---|---|---|---|---|---|---|---|---|---|---|---|---|---|
| | Day -1 | Day 6 | | Day 11 | | Day 25 | | | Day -1 | Day 6 | | Day 11 | | Day 25 | | |
| **Brain Regions** | **Mean ± SE** | **Mean ± SE** | ***p*** | **Mean ± SE** | ***p*** | **Mean ± SE** | ***P*** | | **Mean ± SE** | **Mean ± SE** | ***P*** | **Mean ± SE** | ***p*** | **Mean ± SE** | ***p*** | |
| Amygdala/Piriform complex | 0.53 ± 0.06 | 0.40 ± 0.03 | n.s. | 0.46 ± 0.01 | n.s. | 0.52 ± 0.06 | n.s. | | 0.50 ± 0.02 | 0.44 ± 0.03 | n.s. | 0.44 ± 0.02 | n.s. | 0.46 ± 0.02 | n.s. | |
| Brainstem | 0.67 ± 0.03 | 0.50 ± 0.05 | 0.006 | 0.59 ± 0.02 | 0.004 | 0.63 ± 0.07 | n.s. | | 0.67 ± 0.02 | 0.53 ± 0.03 | 0.001 | 0.59 ± 0.03 | 0.010 | 0.62 ± 0.04 | n.s. | |
| Cerebellum | 0.69 ± 0.02 | 0.63 ± 0.05 | n.s. | 0.76 ± 0.03 | n.s. | 0.78 ± 0.06 | n.s. | | 0.90 ± 0.03 | 0.80 ± 0.05 | 0.039 | 0.83 ± 0.02 | 0.021 | 0.83 ± 0.03 | n.s. | |
| Cingulate cortex | 0.63 ± 0.01 | 0.66 ± 0.04 | n.s. | 0.77 ± 0.04 | 0.022 | 0.92 ± 0.06 | <0.001 | | 0.82 ± 0.06 | 0.75 ± 0.05 | n.s. | 0.73 ± 0.03 | n.s. | 0.73 ± 0.05 | n.s. | |
| Entorhinal cortex | 0.58 ± 0.02 | 0.39 ± 0.03 | <0.001 | 0.45 ± 0.01 | <0.001 | 0.48 ± 0.04 | 0.009 | | 0.50 ± 0.01 | 0.42 ± 0.03 | 0.02 | 0.46 ± 0.02 | 0.008 | 0.46 ± 0.02 | n.s. | |
| Frontal association cortex | 0.91 ± 0.06 | 0.97 ± 0.08 | n.s. | 1.04 ± 0.04 | n.s. | 1.14 ± 0.07 | 0.012 | | 1.18 ± 0.06 | 1.04 ± 0.08 | 0.01 | 1.04 ± 0.04 | 0.006 | 1.08 ± 0.05 | n.s. | |
| Hippocampus | 0.56 ± 0.02 | 0.40 ± 0.03 | <0.001 | 0.47 ± 0.01 | 0.002 | 0.53 ± 0.06 | n.s. | | 0.56 ± 0.02 | 0.46 ± 0.02 | <0.001 | 0.51 ± 0.02 | 0.033 | 0.52 ± 0.02 | 0.042 | |
| Hypothalamus | 0.68 ± 0.03 | 0.41 ± 0.03 | <0.001 | 0.48 ± 0.02 | <0.001 | 0.58 ± 0.06 | n.s. | | 0.50 ± 0.02 | 0.43 ± 0.03 | 0.018 | 0.46 ± 0.02 | n.s. | 0.44 ± 0.02 | 0.018 | |
| Insular cortex | 0.50 ± 0.02 | 0.41 ± 0.03 | 0.008 | 0.42 ± 0.01 | <0.001 | 0.51 ± 0.05 | n.s. | | 0.54 ± 0.02 | 0.45 ± 0.02 | 0.003 | 0.47 ± 0.02 | <0.001 | 0.48 ± 0.02 | <0.001 | |
| Medial Prefrontal cortex | 0.61 ± 0.03 | 0.66 ± 0.04 | n.s. | 0.77 ± 0.02 | <0.001 | 0.88 ± 0.07 | <0.001 | | 0.89 ± 0.05 | 0.76 ± 0.04 | 0.003 | 0.78 ± 0.03 | 0.008 | 0.79 ± 0.03 | <0.001 | |
| Motor/Somatosensory cortex | 0.66 ± 0.03 | 0.57 ± 0.03 | 0.039 | 0.65 ± 0.03 | n.s. | 0.74 ± 0.04 | n.s. | | 0.72 ± 0.05 | 0.65 ± 0.05 | n.s. | 0.64 ± 0.03 | n.s. | 0.60 ± 0.04 | 0.039 | |
| Orbitofrontal cortex | 0.64 ± 0.02 | 0.69 ± 0.04 | n.s. | 0.76 ± 0.02 | <0.001 | 0.90 ± 0.07 | 0.001 | | 0.92 ± 0.03 | 0.76 ± 0.04 | <0.001 | 0.80 ± 0.03 | <0.001 | 0.82 ± 0.03 | <0.001 | |
| Striatum | 0.49 ± 0.02 | 0.36 ± 0.02 | <0.001 | 0.42 ± 0.01 | <0.001 | 0.47 ± 0.04 | n.s. | | 0.50 ± 0.02 | 0.41 ± 0.02 | <0.001 | 0.45 ± 0.02 | 0.006 | 0.44 ± 0.02 | <0.001 | |

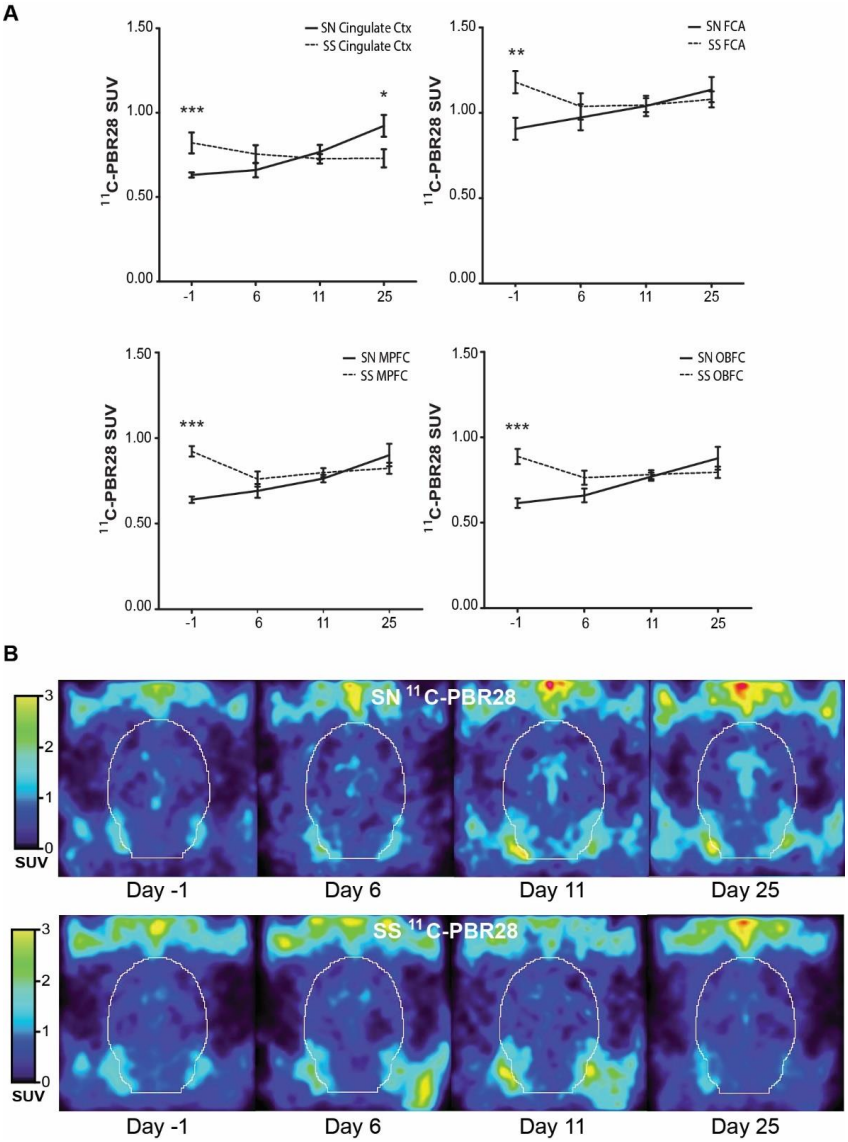


**Figure 5: A** - Graphical representation of the opposite behavior between SN and SS rats regarding $^{11}$C-PBR28 uptake in the cingulate cortex, frontal cortex association (FCA), medial prefrontal cortex (MPFC) and orbitofrontal cortex (OBFC) on day -1, 6, 11 and 25. *$p$<0.05, **$p$<0.01 and ***$p$<0.001. **B:** Representative $^{11}$C-PBR28 PET images from SN and SS rats on day -1, 6, 11 and 25.

Conversely, within-group comparisons in SS rats only showed diminished $^{11}$C-PBR28 tracer uptake in multiple brain regions. Immediately after RSD (day 6), a significant decrease was found in the brainstem (-21%, $p$=0.001), cerebellum (-11%, $p$=0.039), entorhinal cortex (-16%, $p$=0.02), FCA (-12%, $p$=0.01), hippocampus (-18%, $p$<0.001), hypothalamus (-14%, $p$=0.018), insular cortex (-17%, $p$=0.003), MPFC (-15%,

*p*=0.003), OBFC (-17%, *p*<0.001) and striatum (-18%, *p*<0.001). On day 11, a similar decreased uptake pattern as on day 6 was observed. On day 25, lower $^{11}$C-PBR28 uptake than at baseline was still observed in the hippocampus (-7%, *p*=0.042), hypothalamus (-12%, *p*=0.018), insular cortex (-11%, *p*<0.001), MPFC (-11%, *p*<0.001), motor / somatosensory cortex (-17%, *p*=0.039), OBFC (-11%, *p*<0.001) and striatum (-10%, *p*<0.001). RSD did not cause a significant increase in $^{11}$C-PBR28 uptake in any brain region of SS rat. The opposite pattern of $^{11}$C-PBR28 uptake over time in the cingulate cortex, FCA, MPFC and OBFC between SN and SS rats is depicted in Fig. 5. When investigating whether the $^{11}$C-PBR28 uptake was related to the observed behavioral outcomes, no correlations were found at all.

*RSD induces increased levels of IL-1β and IL-10 in the brain of SN rats*

On day 25, significantly higher levels of IL-1β were observed in the cerebellum (SN: 618 pg/mg, IQR 352-959 *vs.* SS: 382 pg/mg, IQR 287-458, *p*=0.036), frontal cortex (SN: 601 pg/mg, IQR 316-796 *vs*. SS: 269 pg/mg, IQR 243–318, *p*=0.003), hippocampus (SN: 614 pg/mg, IQR 478-955 *vs*. SS: 295 pg/mg, IQR 259-387, *p*=0.004) (Fig.6-A) and in the parietal/temporal/occipital (P/T/O) cortex (SN: 576 pg/mg, IQR 467-947 *vs*. SS: 268 pg/mg, IQR 257-315, p=0.007) (Fig. 6-C) of SN rats than in SS rats. Also, IL-1β levels strongly correlated in a positive manner with $^{11}$C-PBR28 uptake in the cingulate cortex of SN rats ($r_s$=0.94, *p*=0.005) (Fig. 6-D). No significant between-group differences in IL-6 levels were observed in any of the investigated brain regions. However, a trend towards significance was observed when comparing the levels of IL-6 in the cerebellum between SN and SS rats (SN: 2730 pg/mg, IQR 1878-4205 *vs*. SS: 1791 pg/mg, IQR 1134-2196, *p*=0.068). Moreover, IL-6 levels in the cerebellum of SN rats positively correlated with $^{11}$C-PBR28 uptake ($r_s$=0.86, *p*=0.014) (Fig. 6-E). Due to technical issues, IL-10 levels were only measured in the P/T/O cortex. SN rats presented significantly higher levels of IL-10 in the P/T/O cortex (SN: 867 pg/mg, IQR 784-1547 *vs*. SS: 473 pg/mg, IQR 351-579, *p*=0.002) than SS rats.

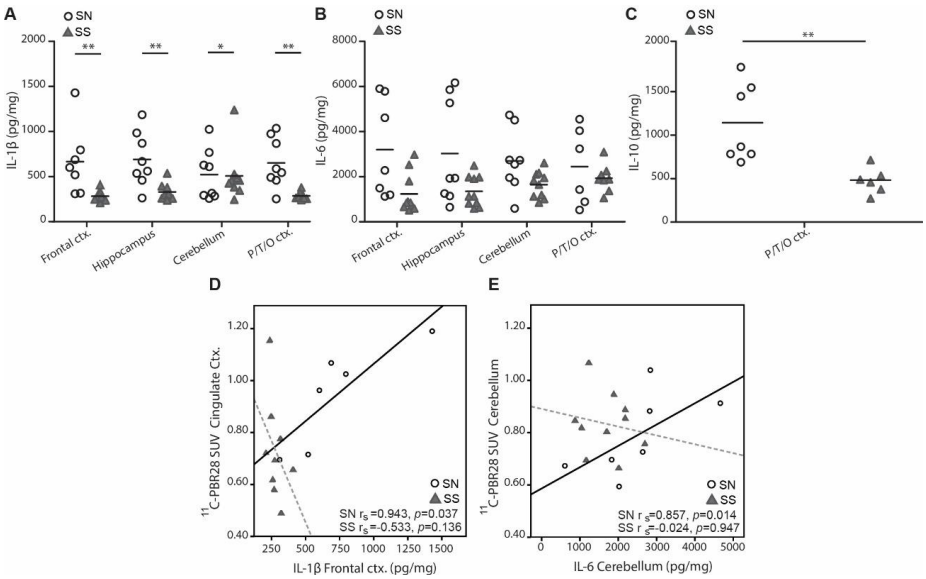


**Figure 6 – A:** Pro-inflammatory cytokines IL-1β and **B:** IL-6 levels in the frontal cortex, hippocampus, cerebellum and parietal/temporal/occipital cortex (P/T/O ctx.) of SN and SS rats. **C:** Anti-inflammatory cytokine IL-10 levels in the P/T/O ctx. between SN and SS rats. *$p$<0.05, **$p$<0.01. **D:** Spearman ($r_s$) correlation between $^{11}$C-PBR28 uptake and IL-1β frontal cortex levels quantified through ELISA in the brain of SN and SS rats on day 25. **E:** Spearman ($r_s$) correlation between $^{11}$C-PBR28 uptake and IL-6 cerebellar levels quantified through ELISA in brain of SN and SS rats on day 25.

*RSD significantly increases corticosterone levels in SN rats, while a recurrence of RSD in SS rats blunts the corticosterone response*

In order to investigate the effect of RSD on corticosterone release, blood samples were taken on day -1, 6, 11 and 25. A significant difference in corticosterone levels between groups was already found at baseline (SN: 240±38 nmol/L vs. SS: 383±56 nmol/L, $p$=0.036). The within-group analysis of corticosterone levels revealed a significant increase in the corticosterone levels in SN rats on day 11 (+61%, $p$=0.015) and 25 (+67%, $p$=0.040), whereas corticosterone levels were significantly decreased in SS rats on day 11 (-28%, $p$=0.036) and 25 (-51%, $p$<0.001), when compared to baseline levels. Consequently, significant between-group differences were found on day 11 (SN: 386±68 nmol/L vs. SS: 275±51 nmol/L, $p$=0.001) and day 25 (SN: 399±75 nmol/L vs. SS: 187±32 nmol/L, $p$<0.001) (Fig. 7-A).

*Corticosterone levels are correlated with increased $^{11}$C-PBR28 uptake in frontal cortical areas of SN rats*

Positive correlations between corticosterone levels and $^{11}$C-PBR28 uptake (SUV) on day 11 were found in the MPFC ($r_s$= 0.74, $p$=0.037) and in the OBFC ($r_s$= 0.88, $p$=0.004) of SN rats (Fig. 7-B and C, respectively). No significant correlations between corticosterone levels and tracer uptake in any other brain region were found at any time point. Also, no significant correlations between corticosterone levels and $^{11}$C-PBR28 uptake were found in any brain region of SS rats at any time point. However, a very strong and positive correlation ($r_s$=1.0, $p$=0.01) between corticosterone levels and the anti-inflammatory cytokine IL-10 was found in the P/T/O cortex of SS rats. When investigating the relationship between $^{18}$F-FDG and corticosterone levels, no significant correlations were found in any brain region of either SN or SS rats.

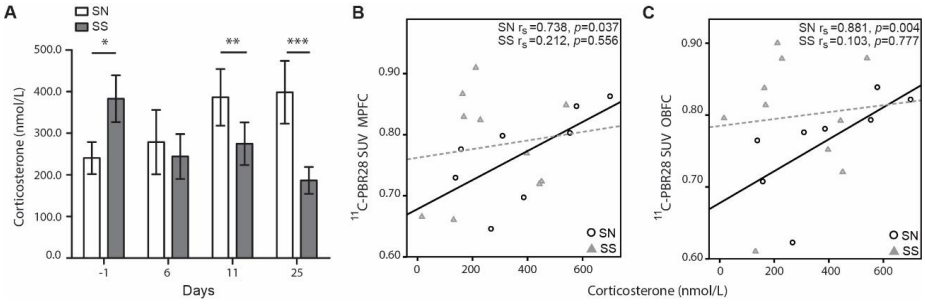


**Figure 7 – A:** Corticosterone levels were altered in a different manner in SN as compared to SS rats. A between-group difference was already apparent at baseline, with SS rats displaying higher corticosterone levels than SN rats ($p$<0.05). Corticosterone levels increased over time in SN rats, being significantly higher than SS rats on day 11 ($p$<0.01) and 25 ($p$<0.001). *$p$<0.05, **$p$<0.01 and ***$p$<0.001. **B**: Spearman correlation ($r_s$) between $^{11}$C-PBR28 uptake (SUV) in the medial prefrontal cortex (MPFC) and corticosterone levels (nmol/L) on day 11 for SN and SS rats. **C:** Spearman correlation ($r_s$) between $^{11}$C-PBR28 uptake (SUV) in the orbitofrontal cortex (OBFC) and corticosterone levels (nmol/L) on day 11 for SN and SS rats.

## Discussion

Chronic stress may have long-lasting effects even after the stressor has been eliminated. So far, the cognitive and behavioral effects of RSD, as a model for psychosocial stress, have only been evaluated shortly after the stressful paradigm. In the present study, we demonstrated that a previous exposure to RSD during adolescence moderates glial activation, brain cytokine and corticosterone responses after a second exposure to the stressful paradigm in aged rats. Moreover, previous exposure to RSD provoked stress-induced depressive-like behavior in SS rats. In contrast, SN rats exposed to RSD had

increased levels of glial activation, production of pro-inflammatory cytokines and higher levels of corticosterone. RSD at old age induced a decrease in brain metabolism and anxiety-like behavior, irrespective of previous exposure to the psychosocial stressor.

The effects of a previous exposure to a stressful condition were already apparent in the body weight measurements during the exposure of the aged rats to RSD. SS rats lost significantly more weight during the 5-day RSD protocol than SN rats. However, from experimental day 4 onwards, both groups changed body weight at the same rate. Behaviourally, SS rats had a more exacerbated reaction to the recurrence of the stressful exposure. While both groups demonstrated anxiety-like behaviour and decreased locomotor activity in the OF test, only SS rats presented anhedonic-like behaviour. The absence of anhedonic behaviour in SN rats adds to the hypothesis that the adult brain is more resilient to stress-induced behavioural alterations than the adolescent brain (26). The previous exposure of SS rats to RSD during adolescence mainly affected areas linked with reward, such as the PFC and OBFC (7). Priming may have made these regions more vulnerable and therefore the secondary stressful stimuli might have provoked a more exacerbated depressive-like response. These results seem to be in agreement with the clinical observation that a history of stress exposures during adolescence can be a precursor to depression in adulthood (51). Previous exposure to RSD did not affect cognition in the NOR test, in accordance with other studies that evaluated long-term memory impairment in a rodent stress model (22; 52).

RSD significantly reduced brain glucose metabolism ($^{18}$F-FDG uptake) in both groups, although with different temporal patterns. SS rats showed a large global decrease in glucose metabolism on day 11, whereas SN rats presented a subtle decrease in glucose metabolism on day 25. Consequently, SS rats displayed lower global $^{18}$F-FDG uptake on day 11 than SN rats. The reduction in brain glucose metabolism can be considered as a surrogate marker of brain activity and thus seems to reflect the reduction in general activity (depressive-like behaviour) observed after RSD. In general, these findings are in accordance with the reduced brain glucose metabolism observed in patients with MDD (11–14)

Our most interesting finding was the opposite glial response to stress between groups, as demonstrated by $^{11}$C-PBR28 PET and brain cytokines levels. Baseline measurements showed higher $^{11}$C-PBR28 uptake (indicative of glial activation) in the cerebellum, cingulate cortex, FCA, MPFC, and OBFC of SS rats than in SN rats. This suggests that exposure to RSD during adolescence primed glial cells (53; 54), inducing

an increased pro-inflammatory profile during ageing. Increasing glial activation during healthy ageing has already been demonstrated both in rodents (55) and humans (56), but priming of microglia by RSD appears to exacerbate the neuroinflammatory profile during ageing. After exposure of aged SN rats to RSD, an increase in tracer uptake was found in the cingulate cortex, MPFC, and OBFC, which persisted until the end of the study. This data is in accordance with glial activation following RSD demonstrated in adolescent rats (22). These results are also in line with recent clinical findings that indicate increased TSPO expression in the prefrontal cortex and cingulate cortex of MDD patients (24; 57). $^{11}$C-PBR28 uptake in the cingulate cortex of SN rats correlated with IL-1β levels, suggesting an important role of the cingulate cortex in the induction of depressive-behaviour after exposure to stressful events (58). Interestingly, SS rats demonstrated persistently decreased $^{11}$C-PBR28 uptake in response to the recurrence of RSD in several brain regions such as the entorhinal cortex, FCA, hippocampus, hypothalamus, insular cortex, MPFC, OBFC, and striatum. This reversed glial response to a recurrence of stressful stimuli might be considered as either an adaptive or maladaptive response to recurrent stress, highlighting the need for further research to unveil such phenomena. As an adaptive approach, blunting of glial response might be considered as a protective mechanism against hyperactivity of the immune system (59). Decreased microglial activation upon repeated stimuli has recently been described as a hypo-active tolerant phenotype, characterized by a decreased cytokine response to proinflammatory stimuli (60). In agreement with the described phenotype, our cytokine measurements displayed significantly lower levels of the pro-inflammatory cytokine IL-1β in the cerebellum, frontal cortex, hippocampus and P/T/O cortex of SS rats, as compared to SN rats. The anti-inflammatory cytokine IL-10 was also significantly decreased in SS rats. On the other hand, a maladaptive response refers to the cumulative effects generated after repeated stress exposure (i.e. allostatic overload), leading to an inefficient (neuro)immunological and neuroendocrine response to recurrent RSD (61; 62). Further studies are required to establish the dynamic role of glial cells in these neurobiological responses.

In order to measure the stress reactivity of the HPA axis in SN and SS rats, corticosterone was measured at several time points after RSD. Our measurements demonstrated a differential corticosterone secretion pattern between groups. SN rats showed a significant increase in corticosterone after RSD exposure, which is in agreement with previous studies in adolescent rats that evaluated corticosterone response shortly

after RSD (19; 22; 29). SS rats, on the other hand, had increased corticosterone levels at baseline, which decreased significantly over time. A similar blunted corticosterone response was recently observed in a rat model of chronic unpredictable stress (63). In adult patients with a history of early life stress, blunted cortisol response was also observed after exposure to acute stressors or dexamethasone suppression (64), supporting the hypothesis that previous trauma is able to modulate the neuroendocrine response to subsequent events.

Interestingly, a significant positive correlation was only found between corticosterone levels and $^{11}$C-PBR28 uptake in the MPFC and OBFC of SN rats. No such correlations were found in SS rats. No correlations between corticosterone levels and $^{18}$F-FDG uptake were observed at all. These results suggest that activation of the HPA axis and thus increased corticosterone levels might be involved in glial activation in response to a novel stress exposure (as in SN rats). The lack of correlation in SS rats might suggest that other pathways than HPA axis activation (not investigated in the present article) are involved in the decreased glial response to a recurrence of a stressful stimuli and the associated anhedonic- and anxiety-like behaviour displayed by SS rats.

The present study has some limitations, mainly due to its longitudinal design. First, PET findings were not confirmed by immunohistochemistry of microglia and/or astrocytes alterations. Instead, quantification of pro- and anti-inflammatory levels of cytokines were used as a proxy for glial activation. Second, tracer uptake was measured as SUV, a simple semi-quantitative measure that allows individual monitoring over time (65). In order to obtain a fully quantitative measure of tracer binding to its receptor (e.g. TSPO), the optimal procedure would be to perform kinetic modelling of $^{11}$C-PBR28 kinetics, but this would require a terminal procedure with arterial blood sampling, since no reference region devoid of TSPO is available within the brain. Due to the longitudinal nature of the study, such methodology was not feasible. However, SUV measurements of $^{11}$C-PBR28 uptake were strongly correlated with the volume of distribution ($V_T$) in previous studies (25; 66), suggesting that the SUV can be used to quantify $^{11}$C-PBR28 uptake in order to simplify the imaging procedure while retaining reliable quantitative information.

In conclusion, we have demonstrated for the first time a dampened glial activation after a recurrence of psychosocial stress in aged rats, in conjunction with more severe depressive- and anxiety-like behavior. The immune response in stress-sensitized rats was not correlated with corticosterone levels, pointing towards an uninvestigated pathway that

might either play a protective role that preserves the brain from further detrimental stimuli, or a maladaptive response to the recurrence of stressful stimuli.

**Acknowledgements**

The authors would like to thank Luiza Reali Nazario for the support in the novel object recognition analysis and Natalia M. Peñaranda Fajardo for technical assistance in the biochemical analysis.

**Disclosure / Conflict of interest**

This research did not receive any specific grant from funding agencies in the public, commercial, or not-for-profit sectors. Paula Kopschina Feltes was a fellowship recipient of Coordenação de Aperfeiçoamento de Pessoal de Nível Superior (CAPES). The Authors declare that there is no conflict of interest.

**References**

1. Santarelli S, Lesuis SL, Wang X-D, Wagner K V., Hartmann J, Labermaier C, *et al.* (2014): Evidence supporting the match/mismatch hypothesis of psychiatric disorders. *Eur Neuropsychopharmacol*. 24: 907–918.
2. de Boer SF, Buwalda B, Koolhaas JM (2017): Untangling the neurobiology of coping styles in rodents: Towards neural mechanisms underlying individual differences in disease susceptibility. *Neurosci Biobehav Rev*. 74: 401–422.
3. Williams LM, Debattista C, Duchemin A-M, Schatzberg AF, Nemeroff CB (2016): Childhood trauma predicts antidepressant response in adults with major depression: data from the randomized international study to predict optimized treatment for depression. *Transl Psychiatry*. 6: e799.
4. Yirmiya R, Rimmerman N, Reshef R (2015): Depression as a Microglial Disease. *Trends Neurosci*. 38: 637–658.
5. Dowlati Y, Herrmann N, Swardfager W, Liu H, Sham L, Reim EK, Lanctôt KL (2010): A Meta-Analysis of Cytokines in Major Depression. *Biol Psychiatry*. 67: 446–457.
6. Kopschina Feltes P, Doorduin J, Klein HC, Juárez-Orozco LE, Dierckx RA, Moriguchi-Jeckel CM, de Vries EF (2017): Anti-inflammatory treatment for major depressive disorder: implications for patients with an elevated immune profile and non-responders to standard antidepressant therapy. *J Psychopharmacol*. 31: 1149–1165.
7. Sheth C, McGlade E, Yurgelun-Todd D (2017): Chronic Stress in Adolescents and Its Neurobiological and Psychopathological Consequences: An RDoC Perspective. *Chronic Stress*. 1: 1–22.
8. Perlman WR, Webster MJ, Herman MM, Kleinman JE, Weickert CS (2007): Age-related differences in glucocorticoid receptor mRNA levels in the human brain. *Neurobiol Aging*. 28: 447–458.
9. Buwalda B, Stubbendorff C, Zickert N, Koolhaas JM (2013): Adolescent social stress does not necessarily lead to a compromised adaptive capacity during adulthood: A study on the consequences of social stress in rats. *Neuroscience*. 249: 258–270.
10. Sung K-K, Jang D-P, Lee S, Kim M, Lee S-Y, Kim Y-B, *et al.* (2009): Neural responses in rat brain during acute immobilization stress: a [F-18]FDG micro PET imaging study.

*Neuroimage*. 44: 1074–1080.
11. Su L, Cai Y, Xu Y, Dutt A, Shi S, Bramon E (2014): Cerebral metabolism in major depressive disorder: a voxel-based meta-analysis of positron emission tomography studies. *BMC Psychiatry*. 14: 1–7.
12. Saxena S, Brody AL, Ho ML, Alborzian S, Ho MK, Maidment KM, *et al.* (2001): Cerebral metabolism in major depression and obsessive-compulsive disorder occurring separately and concurrently. *Biol Psychiatry*. 50: 159–170.
13. Martinot J, Hardy P, Feline A (1990): Left prefrontal glucose hypometabolism in the depressed state: a confirmation. *Am J Psychiatry*. 147: 1313–1317.
14. Biver F, Goldman S, Delvenne V, Luxen A, Demaertelaer V, Hubain P, *et al.* (1994): Frontal and Parietal Metabolic Disturbances in Unipolar Depression. *Biol Psychiatry*. 36: 381–388.
15. Anders S, Tanaka M, Kinney DK (2013): Depression as an evolutionary strategy for defense against infection. *Brain Behav Immun*. 31: 9–22.
16. Koolhaas JM, Coppens CM, de Boer SF, Buwalda B, Meerlo P, Timmermans PJA (2013): The Resident-intruder Paradigm: A Standardized Test for Aggression, Violence and Social Stress. *J Vis Exp*. 77: 1–7.
17. Beery AK, Kaufer D (2015): Stress, social behavior, and resilience: Insights from rodents. *Neurobiol Stress*. 1: 116–127.
18. McKim DB, Weber MD, Niraula A, Sawicki CM, Liu X, Jarrett BL, *et al.* (2017): Microglial recruitment of IL-1β-producing monocytes to brain endothelium causes stress-induced anxiety. *Mol Psychiatry*. E-pub ahead of print. DOI: 10.1038/mp.2017.64.
19. Ramirez K, Fornaguera-Trías J, Sheridan JF (2016): Stress-Induced Microglia Activation and Monocyte Trafficking to the Brain Underlie the Development of Anxiety and Depression. *Brain Imaging Behav Neurosci*. pp 155–172.
20. Wohleb ES, Hanke ML, Corona AW, Powell ND, Stiner LM, Bailey MT, *et al.* (2011): β-Adrenergic Receptor Antagonism Prevents Anxiety-Like Behavior and Microglial Reactivity Induced by Repeated Social Defeat. *J Neurosci*. 31: 6277–6288.
21. Wohleb ES, McKim DB, Shea DT, Powell ND, Tarr AJ, Sheridan JF, Godbout JP (2014): Re-establishment of Anxiety in Stress-Sensitized Mice Is Caused by Monocyte Trafficking from the Spleen to the Brain. *Biol Psychiatry*. 75: 970–981.
22. Kopschina Feltes P, de Vries EF, Juarez-Orozco LE, Kurtys E, Dierckx RA, Moriguchi-Jeckel CM, Doorduin J (2017): Repeated social defeat induces transient glial activation and brain hypometabolism: A positron emission tomography imaging study. *J Cereb Blood Flow Metab*. E-pub ahead of print. DOI: 10.1177/0271678X17747189.
23. Wohleb ES, Franklin T, Iwata M, Duman RS (2016): Integrating neuroimmune systems in the neurobiology of depression. *Nat Rev Neurosci*. 17: 497–511.
24. Setiawan E, Wilson AA, Mizrahi R, Rusjan PM, Miler L, Rajkowska G, *et al.* (2015): Role of Translocator Protein Density, a Marker of Neuroinflammation, in the Brain During Major Depressive Episodes. *JAMA Psychiatry*. 72: E1–E8.
25. Parente A, Feltes PK, Vallez Garcia D, Sijbesma JWA, Moriguchi Jeckel CM, Dierckx RAJO, *et al.* (2016): Pharmacokinetic Analysis of 11C-PBR28 in the Rat Model of Herpes Encephalitis: Comparison with (R)-11C-PK11195. *J Nucl Med*. 57: 785–791.
26. Buwalda B, Geerdink M, Vidal J, Koolhaas JM (2011): Social behavior and social stress in adolescence: A focus on animal models. *Neurosci Biobehav Rev*. 35: 1713–1721.
27. Ma X, Jiang D, Jiang W, Wang F, Jia M, Wu J, *et al.* (2011): Social Isolation-Induced Aggression Potentiates Anxiety and Depressive-Like Behavior in Male Mice Subjected to Unpredictable Chronic Mild Stress. *PLoS One*. 6: e20955.
28. Visser AKD, Meerlo P, Ettrup A, Knudsen GM, Bosker FJ, den Boer JA, *et al.* (2014): Acute social defeat does not alter cerebral 5-HT 2A receptor binding in male Wistar rats. *Synapse*. 68: 379–386.
29. Patki G, Solanki N, Atrooz F, Allam F, Salim S (2013): Depression, anxiety-like behavior and memory impairment are associated with increased oxidative stress and inflammation in a rat model of social stress. *Brain Res*. 1539: 73–86.
30. Razzoli M, Domenici E, Carboni L, Rantamaki T, Lindholm J, Castrén E, Arban R (2011): A role for BDNF/TrkB signaling in behavioral and physiological consequences of social defeat

stress. *Genes, Brain Behav*. 10: 424–433.
31. Liu L, Zhou X, Zhang Y, Liu Y, Yang L, Pu J, *et al.* (2016): The identification of metabolic disturbances in the prefrontal cortex of the chronic restraint stress rat model of depression. *Behav Brain Res*. 305: 148–156.
32. Dere E, Huston JP, De Souza Silva MA (2007): The pharmacology, neuroanatomy and neurogenetics of one-trial object recognition in rodents. *Neurosci Biobehav Rev*. 31: 673–704.
33. Elizalde N, Gil-Bea FJ, Ramírez MJ, Aisa B, Lasheras B, Del Rio J, Tordera RM (2008): Long-lasting behavioral effects and recognition memory deficit induced by chronic mild stress in mice: effect of antidepressant treatment. *Psychopharmacology (Berl)*. 199: 1–14.
34. Hovens IB, van Leeuwen BL, Nyakas C, Heineman E, van der Zee EA, Schoemaker RG (2015): Prior infection exacerbates postoperative cognitive dysfunction in aged rats. *Am J Physiol - Regul Integr Comp Physiol*. 309: R148–R159.
35. Hurley LL, Akinfiresoye L, Kalejaiye O, Tizabi Y (2014): Antidepressant effects of resveratrol in an animal model of depression. *Behav Brain Res*. 268: 1–7.
36. Wong K-P, Sha W, Zhang X, Huang S-C (2011): Effects of Administration Route, Dietary Condition, and Blood Glucose Level on Kinetics and Uptake of 18F-FDG in Mice. *J Nucl Med*. 52: 800–807.
37. Vállez García D, Dierckx RAJO, Doorduin J (2016): Three months follow-up of rat mild traumatic brain injury: a combined [18F]FDG and [11C]PK11195 PET study. *J Neurotrauma*. 33: 1855-1865.
38. Vállez Garcia D, Casteels C, Schwarz AJ, Dierckx RAJO, Koole M, Doorduin J (2015): A Standardized Method for the Construction of Tracer Specific PET and SPECT Rat Brain Templates: Validation and Implementation of a Toolbox. (J.-C. Baron, editor) *PLoS One*. 10: e0122363.
39. Boellaard R, Delgado-Bolton R, Oyen WJ, Giammarile F, Tatsch K, Eschner W, *et al.* (2015): FDG PET/CT: EANM procedure guidelines for tumour imaging: version 2.0. *Eur J Nucl Med Mol Imaging*. 42: 328–354.
40. Weber MD, Godbout JP, Sheridan JF (2017): Repeated Social Defeat, Neuroinflammation, and Behavior: Monocytes Carry the Signal. *Neuropsychopharmacology*. 42: 46–61.
41. Kim Y-K, Won E (2017): The influence of stress on neuroinflammation and alterations in brain structure and function in major depressive disorder. *Behav Brain Res*. 329: 6–11.
42. Phillips JR, Hewedi DH, Eissa AM, Moustafa AA (2015): The Cerebellum and Psychiatric Disorders. *Front Public Heal*. 3: 1–8.
43. Wei K, Xue H, Guan Y, Zuo C, Ge J, Zhang H, *et al.* (2016): Analysis of glucose metabolism of 18F-FDG in major depression patients using PET imaging: Correlation of salivary cortisol and α-amylase. *Neurosci Lett*. 629: 52–57.
44. Hinwood M, Tynan RJ, Day TA, Walker FR (2011): Repeated Social Defeat Selectively Increases FosB Expression and Histone H3 Acetylation in the Infralimbic Medial Prefrontal Cortex. *Cereb Cortex*. 21: 262–271.
45. Yu T, Guo M, Garza J, Rendon S, Sun X-L, Zhang W, Lu X-Y (2011): Cognitive and neural correlates of depression-like behaviour in socially defeated mice: an animal model of depression with cognitive dysfunction. *Int J Neuropsychopharmacol*. 14: 303–317.
46. Marx C, Lex B, Calaminus C, Hauber W, Backes H, Neumaier B, *et al.* (2012): Conflict Processing in the Rat Brain: Behavioral Analysis and Functional μPET Imaging Using [18F]Fluorodeoxyglucose. *Front Behav Neurosci*. 6: 1–12.
47. Lehnert W, Gregoire M-C, Reilhac A, Meikle SR (2012): Characterisation of partial volume effect and region-based correction in small animal positron emission tomography (PET) of the rat brain. *Neuroimage*. 60: 2144–2157.
48. Hardin JW, Hilbe JM (2013): *Generalized Estimating Equations*, Second edition. New York: Chapman & Hall / CRC Press.
49. Streiner DL (2015): Best (but oft-forgotten) practices: The multiple problems of multiplicity-whether and how to correct for many statistical tests. *Am J Clin Nutr*. 102: 721–728.
50. Holm S (1979): A Simple Sequentially Rejective Multiple Test Procedure. *Scand J Stat*. 6: 65–70.

51. McCormick CM, Green MR, Simone JJ (2017): Translational relevance of rodent models of hypothalamic-pituitary-adrenal function and stressors in adolescence. *Neurobiol Stress*. 6: 31–43.
52. McKim DB, Niraula A, Tarr AJ, Wohleb ES, Sheridan JF, Godbout JP (2016): Neuroinflammatory Dynamics Underlie Memory Impairments after Repeated Social Defeat. *J Neurosci*. 36: 2590–2604.
53. Frank MG, Watkins LR, Maier SF (2013): Stress-induced glucocorticoids as a neuroendocrine alarm signal of danger. *Brain Behav Immun*. 33: 1–6.
54. Frank MG, Weber MD, Watkins LR, Maier SF (2015): Stress sounds the alarmin: The role of the danger-associated molecular pattern HMGB1 in stress-induced neuroinflammatory priming. *Brain Behav Immun*. 48: 1–7.
55. Liu B, Le KX, Park M, Wang S, Belanger AP, Dubey X, *et al.* (2015): In Vivo Detection of Age- and Disease-Related Increases in Neuroinflammation by 18 F-GE180 TSPO MicroPET Imaging in Wild-Type and Alzheimer's Transgenic Mice. *J Neurosci*. 35: 15716–15730.
56. Schuitemaker A, van der Doef TF, Boellaard R, van der Flier WM, Yaqub M, Windhorst AD, *et al.* (2012): Microglial activation in healthy aging. *Neurobiol Aging*. 33: 1067–1072.
57. Holmes SE, Hinz R, Conen S, Gregory CJ, Matthews JC, Anton-Rodriguez JM, *et al.* (2018): Elevated Translocator Protein in Anterior Cingulate in Major Depression and a Role for Inflammation in Suicidal Thinking: A Positron Emission Tomography Study. *Biol Psychiatry*. 83: 61–69.
58. Lutz P-E, Tanti A, Gasecka A, Barnett-Burns S, Kim JJ, Zhou Y, *et al.* (2017): Association of a History of Child Abuse With Impaired Myelination in the Anterior Cingulate Cortex: Convergent Epigenetic, Transcriptional, and Morphological Evidence. *Am J Psychiatry*. 174: 1185–1194.
59. Schaafsma W, Zhang X, van Zomeren KC, Jacobs S, Georgieva PB, Wolf SA, *et al.* (2015): Long-lasting pro-inflammatory suppression of microglia by LPS-preconditioning is mediated by RelB-dependent epigenetic silencing. *Brain Behav Immun*. 48: 205–221.
60. Eggen BJL, Raj D, Hanisch UK, Boddeke HWGM (2013): Microglial phenotype and adaptation. *J Neuroimmune Pharmacol*. 8: 807–823.
61. McEwen BS (2007): Physiology and Neurobiology of Stress and Adaptation: Central Role of the Brain. *Physiol Rev*. 87: 873–904.
62. Frank MG, Watkins LR, Maier SF (2013): Stress-induced glucocorticoids as a neuroendocrine alarm signal of danger. *Brain Behav Immun*. 33: 1–6.
63. Natarajan R, Forrester L, Chiaia NL, Yamamoto BK (2017): Chronic-Stress-Induced Behavioral Changes Associated with Subregion-Selective Serotonin Cell Death in the Dorsal Raphe. *J Neurosci*. 37: 6214–6223.
64. Yehuda R, Flory JD, Pratchett LC, Buxbaum J, Ising M, Holsboer F (2010): Putative biological mechanisms for the association between early life adversity and the subsequent development of PTSD. *Psychopharmacology (Berl)*. 212: 405–417.
65. Lodge MA (2017): Repeatability of SUV in Oncologic 18 F-FDG PET. *J Nucl Med*. 58: 523–532.
66. Tóth M, Doorduin J, Häggkvist J, Varrone A, Amini N, Halldin C, Gulyás B (2015): Positron Emission Tomography studies with [11C]PBR28 in the Healthy Rodent Brain: Validating SUV as an Outcome Measure of Neuroinflammation. (K. Hashimoto, editor) *PLoS One*. 10: e0125917.